Hindawi
International Journal of Antennas and Propagation
Volume 2019, Article ID 2837315, 10 pages
https://doi.org/10.1155/2019/2837315

Research Article

DOA Estimation for Highly Correlated and Coherent Multipath Signals with Ultralow SNRs

Li Cheng,[1] Yang Li ,[1] Lianying Zou,[1] and Yong Qin[2]

[1]*Hubei Engineering Research Center of Video Image and HD Projection, School of Electrical and Information Engineering, Wuhan Institute of Technology, Wuhan 430205, China*
[2]*School of Information Engineering, Nanchang Institute of Technology, Nanchang 330099, China*

Correspondence should be addressed to Yang Li; 85155288@qq.com

Received 3 April 2019; Accepted 4 September 2019; Published 13 October 2019

Academic Editor: Ana Alejos

In a typical multipath propagation environment, there exists a strong direct path signal accompanying with several weak multipath signals. Due to the strong direct path interference and other masking effects, the Direction-of-Arrival (DOA) of a weak multipath signal is hard to be estimated. In this paper, a novel method is proposed to estimate the DOA of multipath signals with ultralow signal-to-noise ratio (SNR). The main idea is to increase the SNR and signal-to-interference ratio (SIR) of the desired multipath signal in time-delay domain before DOA estimation processing. Firstly, the cross-correlation functions of the direct path signal and the received array signal are calculated. Then, they are combined and constructed to an enhanced array signal. Under certain conditions, the SNR and SIR of the desired signal can be significantly increased. Finally, the DOAs of multipath signals can be estimated by conventional technologies, and the associated time delays can be measured on the DOA-time-shift map. The SNR and SIR gains of the desired signal are analyzed theoretically, and theoretical analysis also indicates that the Cramer–Rao bound can be reduced. Simulation examples are presented to verify the advantages of the proposed method.

1. Introduction

Direction-of-Arrival (DOA) plays an important role in wireless communication, radar, sonar, and other areas. In the past few decades, many methods, such as subspace-based approaches, maximum likelihood methods, and sparse-representation-based methods [1–5] have been studied extensively on this topic.

In some multipath environments, such as ionospheric sounding [6], global navigation satellite system [7], and airborne radar [8], some of the incident signals are highly correlated with each other, and some of them can be coherent. In this scenario, the performance of conventional DOA estimation methods is affected dramatically. For example, the popular subspace-based methods MUltiple SIgnal Classification (MUSIC) fails to span the signal subspace in the case of correlated waves. MUSIC can be extended to be applicable by adopting decorrelation preprocessing, such as the spatial smoothing [9] and Toeplitz approximation techniques [10]. Also, the maximum likelihood methods [11] and sparse-representation-based methods [12] can be applicable to the coherent scenario. However, they do not consider the case that the signal-to-noise ratio (SNR) of the desired multipath signal whose DOA needs to be estimated can be very low, and there exists strong direct path which can mask the adjacent weak path. For example, in passive bistatic radar system, the power difference between the echo signal and direct path signal can be larger than 100 dB, which indicates the signal-to-interference ratio (SIR) of the desired echo signal is very low [13], thus estimating the DOA of echo signal is a challenging problem [14].

In low SNR case, the number of sources is hard to estimate correctly, and the signal subspace may swap with the noise subspace [15]. Some research studies have been conducted: a MUSIC-like DOA estimation method without estimating the number of sources is proposed in [16], its performance holds stable when SNR is low; a sparse representation of array covariance vectors in an overcomplete basis is proposed in [17], which is statistically robust in low SNR cases; a two-stage DOA estimation method for low

SNR signals is proposed in [18], which enhances the angular resolution and estimation accuracy, particularly for the case when the array antenna elements received the low SNR signals; a linear prediction orthogonal propagator method is proposed in [19], which is more robust to the noise, especially in low SNR scenarios. Although these methods improved the performance of DOA estimation in low SNR scenarios, the performance is constrained by the Cramer–Rao bound (CRB). The CRB relates to many factors, such as the number of snapshots, the array aperture, angular separations, and correlations of the signals, no doubt that SNR is one of the most important factors among them.

This work mainly focuses on the DOA estimation for partly correlated or coherent signals with ultralow SNR in multipath environment, and the precondition that a strong direct path signal is included in the multipath is required, or the reference signal is available in advance. To overcome the SNR limitation, we provide a novel method that can enhance the desired multipath signal before the DOA estimation procedure. We realize this goal through four steps: firstly, the direct path signal is obtained by the conventional DOA estimation and beamforming technologies with the received original array signal (OAS); secondly, the cross-correlation of the direct path signal and OAS are calculated, and then they are combined to a single snapshot array signal; thirdly, the single snapshot is extended to multi-snapshots-enhanced array signal (EAS), under certain conditions, the EAS with particular time shift can be enhanced. At last, by using the time-shift scanning and conventional DOA estimation approaches, the DOAs of multipath signals can be estimated and the associated time delays can be measured on a two-dimensional DOA-time-shift map.

The main contributions of the work are as follows: (a) based on the OAS, a new array signal EAS is constructed, in which the desired multipath signal can be enhanced; (b) the SNR gain and SIR gain in the EAS are derived in theory; (c) the DOA and the associated time delay of the multipath signal with ultralow SNR can be estimated or measured with the EAS; (d) the CRB for DOA estimation can be reduced with the proposed method starting with the OAS.

The rest of the paper is organized as follows: The basic signal model and array signal processing are provided in Section 2. The proposed method and its implementation are developed in Section 3. Some simulation examples are presented in Section 4. A brief conclusion appears in Section 5. In the paper, $E[\cdot]$, $(\cdot)^T$, $(\cdot)^H$, $(\cdot)^{-1}$, $|\cdot|$, $\odot$, and superscript * denote the expectation, transpose, Hermitian transpose, inverse, absolute value, Hadamard product, and complex conjugate, respectively. Boldfaced variable denotes matrix or vector.

2. Problem Formulation

2.1. Array Signal Model. Consider a multipath propagation environment, assuming that there is one direct path signal with its SNR significantly larger than other multipath signals, and there is no strong interference with the same frequency. Multipath signals incident on a uniform linear array (ULA) with M omnidirectional antennas, and the source is in the far field of the array. The received array signal can be expressed as [9]

$$\mathbf{x}(k) = \sum_{i=0}^{L} \eta_i s(k + \tau_i)\mathbf{a}_i + \mathbf{n}(k), \tag{1}$$

where k denotes the snapshot point, the number of multipath signals is $L + 1$, the ith multipath signal is with steering vector $\mathbf{a}_i$, η_i denotes amplitude attenuation, and τ_i denotes time delay. Let $i = 0$ represents the direct path; we can make $\eta_0 = 1$ and $\tau_0 = 0$ for reference. Array signal $\mathbf{x}(k)$, steering vector $\mathbf{a}_i$, and array noise $\mathbf{n}(k)$ are $M \times 1$ dimensional complex vector. The signals are stationary Gaussian random process, and the additive noise is a spatially white Gaussian process. The power of direct path signal and noise is σ_s^2 and σ_n^2, respectively, and the power of ith multipath signal is $\eta_i^2\sigma_s^2$. $\mathbf{x}(k)$ is called OAS in the following.

The data covariance matrix can be expressed as $E[\mathbf{x}(k)\mathbf{x}^H(k)]$. Since the actual covariance matrix is unknown in practice, it is often replaced by K snapshots sample data covariance matrix $\mathbf{R} = (1/K)\sum_{k=1}^{K}\mathbf{x}(k)\mathbf{x}^H(k)$. The data covariance matrix can be further expressed in different forms which depend on whether the signals are coherent or not [20].

The eigen decomposition of $\mathbf{R}$ is

$$\mathbf{R} = \sum_{i=1}^{M} \gamma_i \mathbf{u}_i\mathbf{u}_i^H = \mathbf{U}_S\Gamma_S\mathbf{U}_S^H + \mathbf{U}_N\Gamma_N\mathbf{U}_N^H, \tag{2}$$

where γ_i and $\mathbf{u}_i$ are the eigenvalues and the corresponding eigenvectors of $\mathbf{R}$. The eigenvalues are sorted in descending order, $\gamma_1 > \cdots > \gamma_d \gg \gamma_{d+1} = \cdots = \gamma_M = \sigma_n^2$, where d is the number of the distinguishable signals. The eigenvectors corresponding to the largest d eigenvalues span the signal subspace $\mathbf{U}_S = [\mathbf{u}_1, \ldots, \mathbf{u}_d]$, and the other eigenvectors corresponding to the smaller eigenvalues span the noise subspace $\mathbf{U}_N = [\mathbf{u}_{d+1}, \ldots, \mathbf{u}_M]$.

2.2. DOA Estimation. There are numerous methods that can be used to estimate the DOA of directional signal with OAS. One of the classic methods is Capon spatial spectrum, which is calculated by

$$P_{\text{Capon}}(\theta) = \frac{1}{\mathbf{a}^H(\theta)\mathbf{R}^{-1}\mathbf{a}(\theta)}, \tag{3}$$

where θ is the DOA of the incident signal. The peaks of the spatial spectrum correspond to the DOAs of distinguishable signals. Although the Capon spatial spectrum is implemented easily, its resolution is limited, and the performance is decreased in low SNR scenarios.

The MUSIC is one of the very popular methods for super-resolution DOA estimation [21], and it is given by

$$P_{\text{MUSIC}}(\theta) = \frac{1}{\mathbf{a}^H(\theta)\mathbf{U}_N\mathbf{U}_N^H\mathbf{a}(\theta)}. \tag{4}$$

Resolution and accuracy of an eigen structure method like MUSIC depend on the number of snapshots, array aperture, angular separations, SNRs, and correlations of the

signals, etc. The CRB provides an algorithm-independent benchmark against which various algorithms can be compared. The stochastic CRB of DOA estimation with OAS is computed as [22]

$$\mathrm{CRB}_{\mathrm{OAS}} = \frac{1}{2K}\left\{\mathrm{Re}\left[\left\{\mathbf{D}^H\left[\mathbf{I} - \mathbf{A}\left(\mathbf{A}^H\mathbf{A}\right)^{-1}\mathbf{A}^H\right]\mathbf{D}\right\} \odot \mathbf{B}_{\mathbf{x}}^T\right]\right\}^{-1}, \tag{5}$$

where $\mathbf{D} = [(\partial \mathbf{a}(\theta_0)/\partial\theta_0), (\partial \mathbf{a}(\theta_1)/\partial\theta_1), \ldots, (\partial \mathbf{a}(\theta_L)/\partial\theta_L)]$, $\mathbf{A} = [\mathbf{a}_0, \mathbf{a}_1, \ldots, \mathbf{a}_L]$, $\mathbf{B}_{\mathbf{x}} = \mathrm{diag}\{\mathrm{SNR}_{\mathrm{OAS}i}\}$, and $\mathrm{SNR}_{\mathrm{OAS}i} = \eta_i^2\sigma_s^2/\sigma_n^2$, $i = 0, 1, \ldots, L$. When other parameters are fixed, the snapshots number K and the SNR (relate to $\mathbf{R}$ and σ_n^2) decide the CRB of OAS. In the following, we will develop a novel method to reduce the CRB with the same OAS.

3. The Proposed Method

3.1. Direct Path Signal Beamforming. Firstly, the direct path signal is required. In some applications, the reference signal such as the pilot signal in communication and the transmitted signal in active radar are priori known, and the direct path signal can be obtained from the reference signal. However, the reference signal is unavailable in many applications. The beamforming technology which is used to filter the directional signal in space can be used to obtain the direct path signal: $y_D(k) = \mathbf{w}^H\mathbf{x}(k)$, where $\mathbf{w}$ is the beamformer's weight vector with its main beam pointing to the DOA of direct path signal. In order to suppress the interference adaptively as well as prevent desired signal self-nulling, the robust adaptive beamforming technologies are suggested to be used. The robust Capon beamformer [23], the robust adaptive beamformer [24], or their improved technologies [25, 26] can be used. After the adaptive beamforming, we assume the obtained direct path signal is pure enough, which means $y_D(k) = \mathbf{w}^H\mathbf{x}(k) \approx s(k)$.

3.2. Array Cross-Correlation. The self-correlation function of $s(k)$ is calculated by

$$c_K(\tau) = \sum_{k=1}^{K} s(k)s^*(k+\tau). \tag{6}$$

When the time shift $\tau = 0$, $c_K(0) \approx K\sigma_s^2$. The self-correlation function has a property that the response is maximized when the time shift τ equals to 0:

$$c_K(0) \geq c_K(\tau). \tag{7}$$

The cross-correlation is a measure of similarity of two series as a function of the displacement of one relative to the other. The discrete form of cross-correlation function of the mth antenna's received signal $x_m(k)$ and direct path signal $y_D(k) \approx s(k)$ is defined as

$$\begin{aligned} r_K^m(\tau) &= \sum_{k=1}^{K} x_m(k)y_D^*(k+\tau) \\ &\approx \sum_{k=1}^{K} x_m(k)s^*(k+\tau), \quad m = 1, 2, \ldots, M. \end{aligned} \tag{8}$$

The peaks of cross-correlation function correspond to the multipath signals that are matched in $\tau = \tau_i$.

Taking a combination of $r_K^m(\tau)$ as $\mathbf{r}_K(\tau) = \left[r_K^1(\tau), r_K^2(\tau), \ldots, r_K^M(\tau)\right]^T$, it can be decomposed as

$$\begin{aligned} \mathbf{r}_K(\tau) &= \sum_{k=1}^{K} \mathbf{x}(k)s^*(k+\tau) \\ &= \sum_{i=0}^{L}\left[\sum_{k=1}^{K} \eta_i s(k+\tau_i)s^*(k+\tau)\right]\mathbf{a}_i + \sum_{k=1}^{K} s^*(k+\tau)\mathbf{n}(k) \\ &= \sum_{i=0}^{L} \eta_i c_K(\tau-\tau_i)\mathbf{a}_i + \sum_{k=1}^{K} s^*(k+\tau)\mathbf{n}(k). \end{aligned} \tag{9}$$

The matrix $\mathbf{r}_K(\tau)$ is $M \times 1$ dimensional, and its form is similar with OAS: the signal component is $\sum_{i=0}^{L}\eta_i c_K(\tau-\tau_i)\mathbf{a}_i$, and the noise component is $\sum_{k=1}^{K} s^*(k+\tau)\mathbf{n}(k)$.

Assuming that the path-1 signal with $(\mathbf{a}_1, \tau_1)$ is the desired signal whose DOA needs to be estimated. If $\tau = \tau_1$, (9) can be decomposed as

$$\mathbf{r}_K(\tau_1) \approx \eta_1 c_K(0)\mathbf{a}_1 + \sum_{i=0,2}^{L} \eta_i c_K(\tau_1-\tau_i)\mathbf{a}_i + \sum_{k=1}^{K} s^*(k+\tau_1)\mathbf{n}(k). \tag{10}$$

Through the Cauchy–Schwarz inequality, we have

$$\left|\sum_{k=1}^{K} s^*(k+\tau_1)n_m(k)\right|^2 \leq \sum_{k=1}^{K}\left|s(k+\tau_1)\right|^2\sum_{k=1}^{K}\left|n_m(k)\right|^2 = K^2\sigma_s^2\sigma_n^2. \tag{11}$$

The SIR and the SNR of the path-1 signal in $\mathbf{x}(k)$ and $\mathbf{r}_K(\tau_1)$ are listed in Table 1. Results show that the SIR and SNR of the path-1 is enhanced in $\mathbf{r}_K(\tau_1)$.

3.3. Enhanced Array Signal. Unfortunately, $\mathbf{r}_K(\tau_1)$ in (10) has only one snapshot; thus, it is hard to use conventional DOA estimation approaches directly. Although there are many methods that can be used to estimate the DOA with a single snapshot, their performance is decreased compared with multisnapshots. In the following, the single snapshot array signal $\mathbf{r}_K(\tau_1)$ is extended to multisnapshots array signal.

Table 1: The comparison of SIR and SNR.

$\mathbf{x}(k) = \sum_{i=0}^{L} \eta_i s(k+\tau_i)\mathbf{a}_i + \mathbf{n}(k)$	$\mathbf{r}_K(\tau_1) \approx \eta_1 c_K(0)\mathbf{a}_1 + \sum_{i=0,2}^{L} \eta_i c_K(\tau_1 - \tau_i)\mathbf{a}_i + \sum_{k=1}^{K} s^*(k+\tau_1)\mathbf{n}(k)$
$\mathrm{SIR} = \eta_1^2/\eta_i^2$	$= [\eta_1^2 c^2(0)]/[\eta_i^2 c^2(\tau_1 - \tau_i)] \geq \eta_1^2/\eta_i^2$
$\mathrm{SNR} = \eta_1^2\sigma_s^2/\sigma_n^2$	$\geq [\eta_1^2 c^2(0)]/[K^2\sigma_s^2\sigma_n^2] = \eta_1^2\sigma_s^2/\sigma_n^2$

As shown in Table 2, the K-length snapshots in $\mathbf{x}(k)$, $k = 1, 2, \ldots, K$ are divided into K_2 uniform segments, and each segment has $K_1 = K/K_2$ subsnapshots.

The cross-correlation of the direct path signal and the array signal for subsnapshots k_2 is

$$\begin{aligned}\mathbf{r}_{K_1}(k_2,\tau) &= \sum_{k=(k_2-1)K_1+1}^{k_2K_1} \mathbf{x}(k)s^*(k+\tau)\\ &= \sum_{i=0}^{L}\left[\sum_{k=(k_2-1)K_1+1}^{k_2K_1} \eta_i s(k+\tau_i)s^*(k+\tau)\right]\mathbf{a}_i\\ &\quad + \sum_{k=(k_2-1)K_1+1}^{k_2K_1} s^*(k+\tau)\mathbf{n}(k)\\ &= \sum_{i=0}^{L} \eta_i c_{K_1}(\tau-\tau_i)\mathbf{a}_i\\ &\quad + \sum_{k=(k_2-1)K_1+1}^{k_2K_1} s^*(k+\tau)\mathbf{n}(k), \quad k_2 = 1,2,\ldots,K_2.\end{aligned} \tag{12}$$

Table 2: Multisnapshots array signal.

Segments	1	2	...	K_2
Subsnapshots	$1\sim K_1$	$K_1+1\sim 2K_1$	...	$1\ (K_2-1)K_1+1\sim K_2\ K_1$
OAS	$x\ (1\sim K_1)$	$x\ (K_1+1\sim 2K_1)$	...	$x[(K_2-1)K_1+1\sim K_2\ K_1]$
Direct path	$s\ (1\sim K_1)$	$s\ (K_1+1\sim 2K_1)$	...	$s[(K_2-1)K_1+1\sim K_2\ K_1]$
Correlation	$r_{K1}\ (1,\tau)$	$r_{K_1}\ (2,\tau)$	...	$r_{K1}\ (K_2,\ \tau)$

Comparing with $\mathbf{r}_K(\tau)$ in (9), the form of $\mathbf{r}_{K_1}(k_2,\tau)$ in (12) is also similar with OAS. We call the combination $[\mathbf{r}_{K_1}(1,\tau), \mathbf{r}_{K_1}(2,\tau), \ldots, \mathbf{r}_{K_1}(K_2,\tau)]$ as the EAS, in which the path with time delay τ is enhanced. The difference and equivalence of OAS in (1) and EAS in (12) are described in Table 3.

Assuming that the snapshots are infinite, according to the discrete time matched filters theory, the noise element at mth antenna is

$$\begin{aligned}E\left\{\left|\sum_{k=1}^{K} s^*(k+\tau_1)n_m(k)\right|^2\right\} &= E\left\{\sum_{k_a=1}^{K}\left[s^*(k_a+\tau_1)n_m(k_a)\right]\sum_{k_b=1}^{K}\left[s(k_b+\tau_1)n_m^*(k_b)\right]\right\}\\ &= \sum_{k_a=1}^{K}\sum_{k_b=1}^{K}\left[s^*(k_a+\tau_1)s(k_b+\tau_1)\right]E\{n_m(k_a)n_m^*(k_b)\}\\ &= \sum_{k_a=1}^{K}\sum_{k_b=1}^{K}\left[s^*(k_a+\tau_1)s(k_b+\tau_1)\right]\sigma_n^2\delta(k_a,k_b)\\ &= \sigma_n^2\sum_{k=1}^{K}\left|s(k+\tau_1)\right|^2 = K\sigma_s^2\sigma_n^2, \quad m = 1,2,\ldots,M,\end{aligned} \tag{13}$$

where δ is an impulse function. Hence, for finite snapshots, we can make

$$\frac{1}{K_2}\sum_{k_2=1}^{K_2}\left|\sum_{k=(k_2-1)K_1+1}^{k_2K_1} s^*(k+\tau)n_m(k)\right|^2 \approx K_1\sigma_s^2\sigma_n^2. \tag{14}$$

The power of signal in path-i is

$$\begin{aligned}\frac{1}{K_2}\sum_{k_2=1}^{K_2}\left|\sum_{k=(k_2-1)K_1+1}^{k_2K_1} \eta_i s(k+\tau_i)s^*(k+\tau)\right|^2 &= \frac{\eta_i^2}{K_2}\sum_{k_2=1}^{K_2} c_{K_1}^2(\tau-\tau_i)\\ &= \eta_i c_{K_1}^2(\tau-\tau_i).\end{aligned} \tag{15}$$

If $\tau = \tau_1$, the relationship of SIR and SNR in the OAS and EAS are

Table 3: Comparison of OAS and EAS.

	$\mathbf{x}(k)$	$\mathbf{r}_{K_1}(k_2,\tau)$
Path-i array signal	$\eta_i s(k+\tau_i)\mathbf{a}_i$	$\sum_{k=(k_2-1)K_1+1}^{k_2K_1}\eta_i s(k+\tau_i)s^*(k+\tau)\mathbf{a}_i$
Array noise	$\mathbf{n}(k)$	$\sum_{k=(k_2-1)K_1+1}^{k_2K_1}s^*(k+\tau)\mathbf{n}(k)$
Snapshot sequence	$k=1,\ldots,K$	$k_2=1,2,\ldots,K_2$

$$\mathrm{SIR}_{\mathrm{EAS}}=\frac{\eta_1^2c_{K_1}^2(0)}{\eta_i^2c_{K_1}^2(\tau_1-\tau_i)}=\left[\frac{c_{K_1}(0)}{c_{K_1}(\tau_1-\tau_i)}\right]^2\mathrm{SIR}_{\mathrm{OAS}},\quad(16)$$

$$\mathrm{SNR}_{\mathrm{EAS}}\approx\frac{\eta_1^2c_{K_1}^2(0)}{K_1\sigma_s^2\sigma_n^2}=\frac{\eta_1^2K_1^2\sigma_s^4}{K_1\sigma_s^2\sigma_n^2}=K_1\frac{\eta_1^2\sigma_s^2}{\sigma_n^2}=K_1\mathrm{SNR}_{\mathrm{OAS}}.\quad(17)$$

Hence, compared with the OAS, the SIR in EAS is enhanced with $[c_{K_1}(0)/c_{K_1}(\tau_1-\tau_i)]^2$ times, and the SNR in EAS is enhanced with K_1 times. Notice that the subsnapshots can be set partly overlapped, and then the snapshots K_2 or the SNR gain K_1 can be further increased.

It is worth noting that the noise $\sum_{k=(k_2-1)K_1+1}^{k_2K_1}s^*(k+\tau)\mathbf{n}(k)$ may not be white. However, in the detection and estimation theory, if the SNR is high, the noise covariance matrix can be assumed to be inappreciable [27]. In EAS, the SNR of the desired signal has been increased about K_1 times, which can be extremely large; hence, we can treat the noise in EAS as white noise for simplification.

3.4. CRB Analysis. There are many existing methods which can be used to estimate the DOAs of multipath signals with EAS. Because the array signal structures in OAS and EAS are similar, the CRB for DOA estimation with EAS is similar with (5)

$$\mathrm{CRB}_{\mathrm{EAS}}=\frac{1}{2K_2}\left\{\mathrm{Re}\left[\left\{\mathbf{D}^H\left[\mathbf{I}-\mathbf{A}\left(\mathbf{A}^H\mathbf{A}\right)^{-1}\mathbf{A}^H\right]\mathbf{D}\right\}\odot\mathbf{B}_{\mathbf{r}}^T\right]\right\}^{-1},\quad(18)$$

where $\mathbf{B}_r=\mathrm{diag}\{\mathrm{SNR}_{\mathrm{EAS}i}\}$, $i=0,1,\ldots,L$. To compute the CRB of a single path-i, we can set $\mathrm{SNR}_{\mathrm{EAS}i}=K_1\mathrm{SNR}_{\mathrm{OAS}i}$. Comparing the $\mathrm{CRB}_{\mathrm{EAS}}$ and the $\mathrm{CRB}_{\mathrm{OAS}}$, although the snapshots number $K_2<K$, the SNR satisfies $\mathrm{SNR}_{\mathrm{EAS}i}>\mathrm{SNR}_{\mathrm{OAS}i}$. Therefore, the $\mathrm{CRB}_{\mathrm{EAS}}$ can be lower than $\mathrm{CRB}_{\mathrm{OAS}}$ under certain conditions.

3.5. Spatial Spectrum Estimation. The MUSIC approach is used to estimate the spatial spectrum of multipath signals. The data covariance matrix of EAS is

$$\mathbf{R}_\tau=\frac{1}{K_2}\sum_{k_2=1}^{K_2}\mathbf{r}(k_2,\tau)\mathbf{r}^H(k_2,\tau).\quad(19)$$

Taking the eigenvalue decomposition of $\mathbf{R}_t=\mathbf{E}_S\mathbf{\Lambda}_S\mathbf{E}_S^H+\mathbf{E}_N\mathbf{\Lambda}_N\mathbf{E}_N^H$, where $\mathbf{E}_S$ and $\mathbf{E}_N$ are the signal subspace and noise subspace, respectively. When $\tau=\tau_i$, since the SIR is enlarged in EAS, which indicates other paths are attenuated, it is foreseeable that there are two signals having the same lager power: the path-i signal and the direct path signal. Hence, it is reasonable to set the dimension of $\mathbf{E}_N$ to $M-2$. When $\tau\neq\tau_i$, the $M-2$ dimensional noise subspace may cause another false alarm peak; fortunately, it is so low that can be omitted. Therefore, the dimension of $\mathbf{E}_N$ can be set equal to $M-2$ directly.

Finally, the MUSIC spatial spectrum is calculated by

$$P_{\mathrm{MUSIC}}(\theta,\tau)=\frac{1}{\mathbf{a}^H(\theta)\mathbf{E}_N\mathbf{E}_N^H\mathbf{a}(\theta)}.\quad(20)$$

Assuming the time delays of multipath signals lie between $\tau_{\min}$ and $\tau_{\max}$, the range $(\tau_{\min},\tau_{\max})$ can be divided to discrete time-shift sequences $\tau(1)$, $\tau(2)$,..., and then the spatial spectra with different time-shift sequences are calculated. By stacking all the spatial spectrums along the time shifts, we can obtain a two dimensional DOA-time-shift map. Only if the time shift equals to the time delay of a multipath signal, the weak multipath signal can be enhanced, and a peak corresponding to its DOA will appear on the spatial spectrum. Therefore, the DOA of the ith multipath signal with time delay $\tau=\tau_i$ corresponds to a peak on the DOA-time-shift map. That is, to say, we can estimate the DOAs and measure their associated time delays on the DOA-time-shift map for all the distinguishable multipath signals.

The MUSIC approach can be replaced, and other DOA estimation methods can be used with the EAS, so do the technologies can deal with coherent signals, such as the spatial smoothing technology [9].

3.6. Implementation. The implementation of the proposed method is summarized as follows:

Step 1: estimating the DOA of direct path signal with K-snapshots OAS; any DOA estimation technology is suitable.

Step 2: obtaining the direct path signal with beamforming technology.

Step 3: dividing the K-snapshots OAS and direct path signal into $k_2=1,2,\ldots,K_2$ segments, and each segment has the same length K_1. For each segment, calculating the cross-correlation function of the direct path signal and the OAS by (12).

Step 4: scanning in the time shift to estimate the DOAs with MUSIC approach:

$$\begin{aligned}&\text{For } \tau=\tau(1),\tau(2),\ldots,\\&\mathbf{R}_\tau=\frac{1}{K_2}\sum_{k_2=1}^{K_2}\mathbf{r}(k_2,\tau)\mathbf{r}^H(k_2,\tau),\\&\mathbf{R}_t=\mathbf{E}_S\mathbf{\Lambda}_S\mathbf{E}_S^H+\mathbf{E}_N\mathbf{\Lambda}_N\mathbf{E}_N^H,\\&P(\theta,\tau)=\frac{1}{\mathbf{a}^H(\theta)\mathbf{E}_N\mathbf{E}_N^H\mathbf{a}(\theta)},\\&\text{End.}\end{aligned}\quad(21)$$

The spectral peaks of two-dimensional DOA-time-shift map $P(\theta, \tau)$ are corresponding to the DOAs and associated time delays of multipath signals. Step 4 can be replaced by the MUSIC approach with forward spatial smoothing technology, if coherent multipath signal exists [9]. In case of two coherent signals, the dimension of the noise subspace should be set to $M_s - 3$, where M_s is the dimension of subarrays in the forward spatial smoothing technology.

The computational complexity of the main operations are as follows: (a) beamforming in step 2: $O(M^3)$, if the method in [24] is used; (b) DOA estimation in steps 1 and 4: $O(M^3)$, if the MUSIC is used; and (c) cross-correlation in step 3: $O(K_1 \log K_1)$, if the fast Fourier transform is used.

4. Simulation Examples

In the following simulation examples, a ULA with $M = 16$ antennas and half-wavelength spacing is considered. Assuming each antenna is omnidirectional, the array has been calibrated. The signal is stationary Gaussian random process, and the additive noise is a spatially white Gaussian process. The baseband signal is generated by a complex white noise sequence filtered with a low-pass filter, and the bandwidth is 80 kHz (also 40 kHz in Example 1). The sampling rate is 100 kHz, and the segments number K_2 is 50.

The proposed method is compared with the following three methods: (a) Capon: the Capon spatial spectrum estimator in (3), which is an easy implantation and widely used method; (b) MUSIC: the MUSIC spatial spectrum estimator in (4), which is a well-known super resolution method. (c) OMP-LP: the linear prediction orthogonal propagator method in [19], which is robust to the noise, especially in low SNR scenarios.

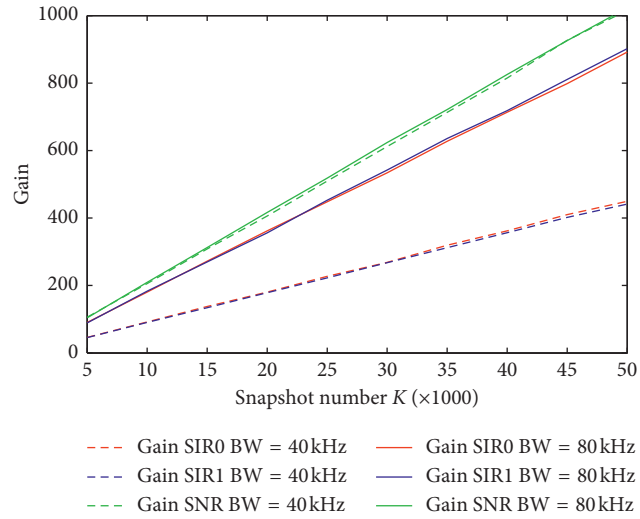

Figure 1: The SIR and SNR gains with different bandwidths and snapshots.

4.1. SIR and SNR Gain. In the first example, we evaluate the influence of signal bandwidth and snapshot number on the gain of SIR and SNR. The SNR and time delay parameters are set the same as Example 2, while the bandwidth is set to 40 kHz and 80 kHz, and the snapshot number K varies from 5000 to 50,000 which means K_1 varies from 100 to 1000. Assume that path-2 is the desired signal and path-0 and path-1 are interference.

The SIR gain is calculated by

$$\text{Gain}_{\text{SIR}i} = \frac{\text{SIR}_{\text{EAS}}}{\text{SIR}_{\text{OAS}}} = \frac{\sum_{k_2=1}^{K_2} \left| \sum_{k=(k_2-1)K_1+1}^{k_2K_1} s(k+\tau_2) s^*(k+\tau_2) \right|^2}{\sum_{k_2=1}^{K_2} \left| \sum_{k=(k_2-1)K_1+1}^{k_2K_1} s(k+\tau_i) s^*(k+\tau_2) \right|^2}, \quad i = 0, 1. \tag{22}$$

The SNR gain is calculated by

$$\text{Gain}_{\text{SNR}} = \frac{\text{SNR}_{\text{EAS}}}{\text{SNR}_{\text{OAS}}} = \frac{\sum_{k_2=1}^{K_2} \left| \sum_{k=(k_2-1)K_1+1}^{k_2K_1} s(k+\tau_2) s^*(k+\tau_2) \right|^2}{\sum_{k_2=1}^{K_2} \left| \sum_{k=(k_2-1)K_1+1}^{k_2K_1} s^*(k+\tau_2) n_1(k) \right|^2} \times \sigma_n^2. \tag{23}$$

Example 1. The SIR and SNR gain simulation.

Figure 1 shows the SIR and SNR gain with different bandwidths and snapshot numbers. Results show that (a) the gain SIR0 and gain SIR1 are almost equal for the same bandwidth and K. It is because the path-0 and path-1 interference are attenuated at almost the same level for the simulated signal. Actually, it can be concluded from (16) that the attenuation level of interference relates to the shape of cross-correlation function of the signal. (b) For the same K, when the bandwidth increases from 40 kHz to 80 kHz, the SIR gain doubled. It is because the value of cross-correlation processing depends on the time bandwidth product; if time K is fixed and bandwidth doubled, the gain doubled correspondingly. (c) The SIR gain and SNR gain increase almost linearly as the snapshot number K increases. (d) The SNR gain is independent of bandwidth, and it is very close to the

theoretical result in (17), which indicates the SNR gain equals to K_1.

4.2. Performance Comparison. In Examples 2 and 3, the multipath signals' parameters are listed in Table 4. Other parameters are: $K = 50000$, $K_1 = 1000$, and $K_2 = 50$.

Example 2. Spatial spectrum comparison.

Figure 2 displays the DOA-time-shift spectrum map. Results show that (a) there is a line at $\theta = 30^\circ$ throughout all the time delays, and it is the residual direct path extended to all the time delays. (b) The peak of the line is with DOA = 30°, and time delay = 0 is corresponding to the direct path signal path-0. (c) The DOAs and their associated time delays of two weak signals path-1 and path-2 can be distinguished correctly and clearly.

Further study shows that the signal with larger bandwidth has higher resolution in time delay. Also, it is shown in Figure 1 that the larger the bandwidth, the larger the SIR gain. However, the MUSIC is a narrowband approach. To apply the proposed method in both the DOA and time delay estimation, the baseband signal should be narrowband compared with the carrier signal, and then the larger the bandwidth, the better the performance, if other parameters are fixed.

To compare the performance with other methods, we extract the maximum value along the time delay 0~1 ms at each direction to construct a one-dimensional spatial spectrum for the proposed method. Results in Figure 3 show that (a) all the methods can estimate the DOA of the direct path signal with SNR = 10 dB, the OMP-LP generates the sharpest peak at the direct path. (b) Both the MUSIC and the OMP-LP and the proposed method can estimate the DOA of path-1 with SNR = −20 dB, and the proposed method generates the sharpest peak. (c) Only the proposed method generates a peak at the DOA of path-2 with SNR = −30 dB.

Example 3. The RMSE comparison.

The SNR of path-2 varies from −40 dB to 0 dB. The root mean square error (RMSE) is calculated for path-2, $\text{RMSE} = \sqrt{(1/1000)\sum_{i=1}^{1000}(\widehat{\theta}_{2i} - \theta_2)^2}$, where θ_2 and $\widehat{\theta}_{2i}$ are the actual and the ith time estimated DOA of path-2, respectively, and $\widehat{\theta}_{2i}$ is obtained by searching the maximum value in $110^\circ : 0.01^\circ : 130^\circ$. 1000 independent runs are performed. Results in Figure 4 show that (a) benefiting from the desired signal is enhanced; the CRB of EAS is lower than the CRB of OAS, and as the SNR becomes lower, the CRB-EAS gets much lower than the CRB-OAS. (b) The RMSE of the proposed method is lower than other methods, especially at much lower SNR scenario. (c) The RMSE of the proposed method is lower than the CRB of OAS.

The SNR of path-2 is fixed at −20 dB, while the number of snapshots K varies from 5000 to 50,000, which indicates $K_2 = 50$, and K_1 varies from 100 to 1000. Results in Figure 5 show that (a) the CRB of EAS is lower than the CRB of OAS. (b) As the number of snapshots increase, the RMSE of the proposed method gets lower, and when the number of subsnapshots K_1 surplus 200, the performance of the proposed method is stable. (c) The RMSE of the proposed method is lower than other methods and is lower than the CRB of OAS when K_1 surplus 150.

Table 4: Simulated parameters for examples 2 and 3.

Multipath	Path-0	Path-1	Path-2
DOA (degree)	60	90	120
SNR (dB)	10	−20	−30
Time delay (ms)	0	0.5	0.8

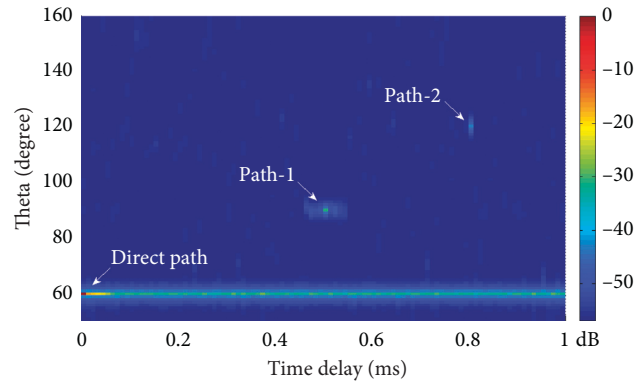

Figure 2: DOA-time-shift spectrum.

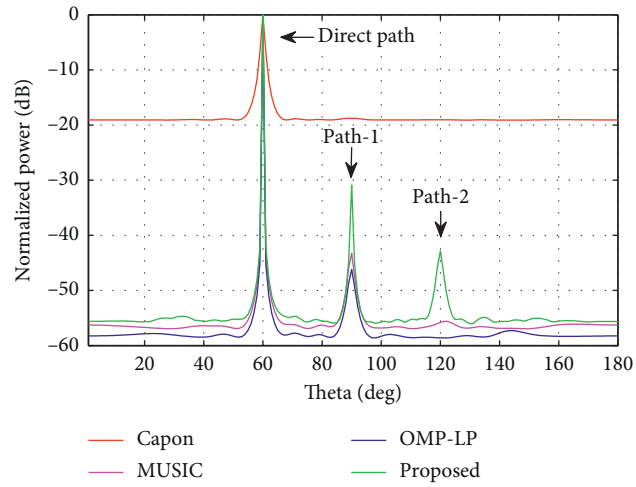

Figure 3: Results comparison for the four methods.

4.3. The Same DOA and Coherent Signals with Ultralow SNRs. In Examples 4 and 5, the multipath signals' parameters are listed in Table 5. Other parameters are: $K = 500000$, $K_1 = 10000$, and $K_2 = 50$. The signals in path-4 and path-5 have the same DOA, and the signals in path-3 and path-4 are coherent.

Example 4. The proposed method applied in ultralow SNR

To our knowledge, the existing DOA estimation methods cannot work at ultralow SNR scenario, such as the SNR is below −40 dB, and there exists a strong direct path at the same time. Figure 6 shows the DOA-time-shift spectrum

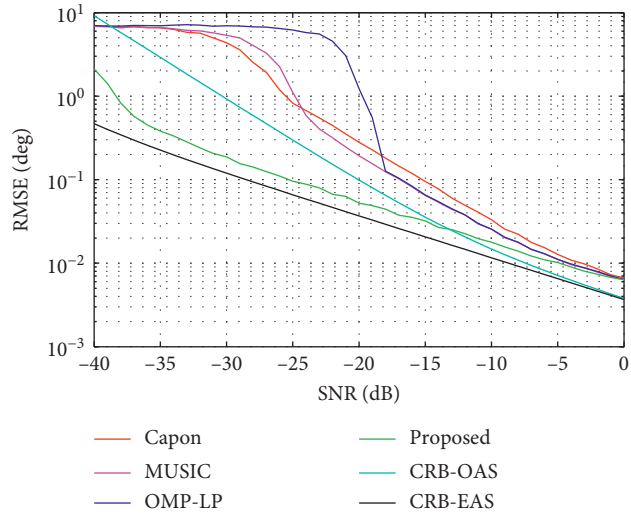

Figure 4: RMSE versus SNR.

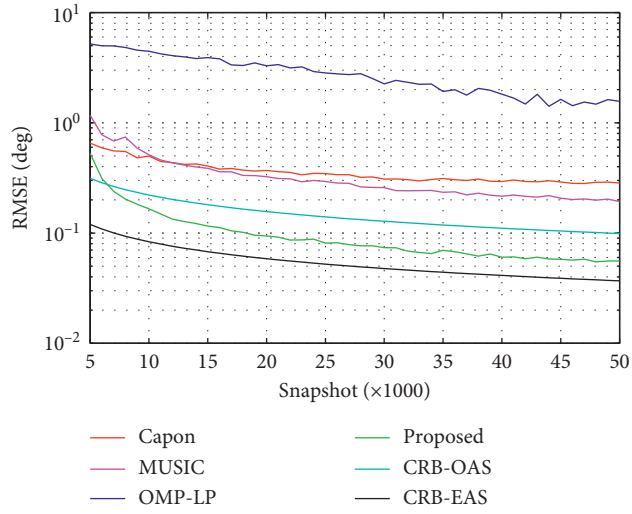

Figure 5: RMSE versus snapshot number.

Table 5: Simulated parameters for Examples 4 and 5.

Multipath	Path-0	Path-1	Path-2	Path-3	Path-4	Path-5	Path-6	Path-7
DOA (degree)	30	70	130	120	100	100	140	80
SNR (dB)	10	−36	−40	−37	−35	−38	−34	−39
Time delay (ms)	0	0.2	0.1	0.4	0.4	0.6	0.8	0.9

calculated by the proposed method. Results show that (a) the DOAs and the associated time delays of path-1, -2, -5, -6, and -7 can be distinguished clearly. (b) Path-3 and path-4 cannot be distinguished because they are coherent.

Example 5. The proposed method with spatial smoothing.

Then, we apply the MUSIC approach with forward spatial smoothing technology [9] in the proposed method. The number of subarrays is set to 2, which means the dimension of subarray is $M - 1 = 15$. The dimension of noise subspace is set to $15 - 3 = 12$. Results in Figure 7 show that the DOAs as well as their associated time delays of two coherent signals path-3 and path-4 can be distinguished correctly and clearly.

5. Conclusion

A novel method was developed to estimate the DOAs of multipath signals with ultralow SNRs. By calculating the cross-correlation function of the direct path signal and the received OAS and then constructing an EAS, the desired multipath signal can be enhanced. The DOA of desired multipath signal can be estimated by the MUSIC approach

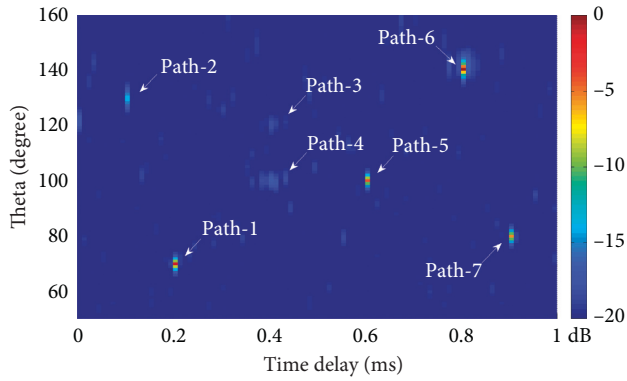

Figure 6: DOA-time-shift spectrum.

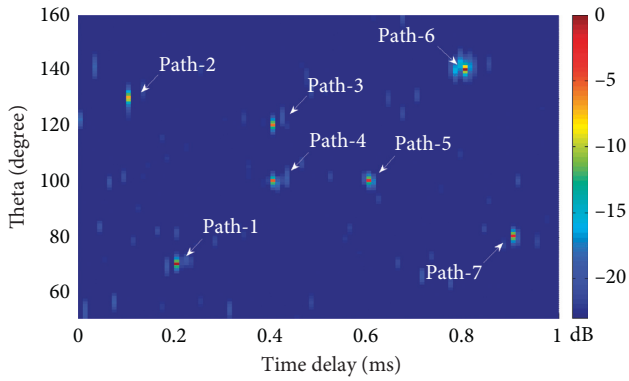

Figure 7: DOA-time-shift spectrum with spatial smoothing.

with the EAS. Theoretical analysis and simulation results indicate that the SNR gain of the desired multipath signal equals to the snapshots number, so the proposed method is able to estimate the DOAs of multipath signals with ultralow SNRs, if the number of snapshots is large enough. Coherent signals with ultralow SNRs can also be measured with spatial smoothing technology by the proposed method. Furthermore, the CRB can be reduced in the EAS.

Data Availability

The software code data used to support the findings of this study are currently under embargo while the research findings are commercialized. Requests for data, 12 months after publication of this article, will be considered by the corresponding author.

Conflicts of Interest

The authors declare that there are no conflicts of interest regarding the publication of this paper.

Acknowledgments

This work was supported by the Scientific Research Foundation of the Hubei Provincial Department of Education under Grant Q20181505 and the Scientific Research Foundation of Wuhan Institute of Technology (no. K201904).

References

[1] J. Dai and H. C. So, "Sparse Bayesian learning approach for outlier-resistant direction-of-arrival estimation," *IEEE Transactions on Signal Processing*, vol. 66, no. 3, pp. 744–756, 2018.

[2] C. Qian, L. Huang, N. D. Sidiropoulos, and H. C. So, "Enhanced PUMA for direction-of-arrival estimation and its performance analysis," *IEEE Transactions on Signal Processing*, vol. 64, no. 16, pp. 4127–4137, 2016.

[3] Y. Wu, A. Leshem, J. R. Jensen, and G. Liao, "Joint pitch and DOA estimation using the ESPRIT method," *IEEE/ACM Transactions on Audio, Speech, and Language Processing*, vol. 23, no. 1, pp. 32–45, 2015.

[4] Z.-M. Liu, Z.-T. Huang, and Y.-Y. Zhou, "An efficient maximum likelihood method for direction-of-arrival estimation via sparse Bayesian learning," *IEEE Transactions on Wireless Communications*, vol. 11, no. 10, pp. 1–11, 2012.

[5] F.-G. Yan, J. Wang, S. Liu, Y. Shen, and M. Jin, "Reduced-complexity direction of arrival estimation using real-valued computation with arbitrary array configurations," *International Journal of Antennas and Propagation*, vol. 2018, Article ID 9695326, 10 pages, 2018.

[6] F. Arikan, O. Koroglu, S. Fidan, O. Arikan, and M. B. Guldogan, "Multipath separation-direction of arrival (MS-DOA) with genetic search algorithm for HF channels," *Advances in Space Research*, vol. 44, no. 6, pp. 641–652, 2009.

[7] X. Chen and Y. Morton, "Iterative subspace alternating projection method for GNSS multipath DOA estimation," *IET Radar, Sonar & Navigation*, vol. 10, no. 7, pp. 1260–1269, 2016.

[8] D. Bonacci, F. Vincent, and B. Gigleux, "Robust DOA estimation in case of multipath environment for a sense and avoid airborne radar," *IET Radar, Sonar & Navigation*, vol. 11, no. 5, pp. 797–801, 2017.

[9] T. J. Shan, M. Wax, and T. Kailath, "On spatial smoothing for direction-of-arrival estimation of coherent signals," *IEEE Transactions on Acoustics, Speech, and Signal Processing*, vol. 33, no. 4, pp. 806–811, 1985.

[10] F. Han and X. Zhang, "An ESPRIT-like algorithm for coherent DOA estimation," *IEEE Antennas and Wireless Propagation Letters*, vol. 4, no. 1, pp. 443–446, 2005.

[11] Y.-H. Choi, "Maximum likelihood estimation for angles of arrival of coherent signals using a coherency profile," *IEEE Transactions on Signal Processing*, vol. 48, no. 9, pp. 2679–2682, 2000.

[12] Z.-M. Liu, Z. Liu, D.-W. Feng, and Z.-T. Huang, "Direction-of-arrival estimation for coherent sources via sparse Bayesian learning," *International Journal of Antennas and Propagation*, vol. 2014, pp. 1–8, 2014.

[13] R. Saini, M. Cherniakov, and V. Lenive, "Direct path interference suppression in bistatic system: DTV based radar," in *Proceedings of the International on Radar Conference, 2003*, pp. 309–314, IEEE, Adelaide, Australia, September 2003.

[14] Y. Li, H. Ma, Y. Wu, L. Cheng, and D. Yu, "DOA estimation for echo signals and experimental results in the AM radio-based passive radar," *IEEE Access*, vol. 6, pp. 73316–73327, 2018.

[15] J. K. Thomas, L. L. Scharf, and D. W. Tufts, "The probability of a subspace swap in the SVD," *IEEE Transactions on Signal Processing*, vol. 43, no. 3, pp. 730–736, 1995.

[16] Y. Zhang and B. P. Ng, "MUSIC-like DOA estimation without estimating the number of sources," *IEEE Transactions on Signal Processing*, vol. 58, no. 3, pp. 1668–1676, 2010.

[17] J. Yin and T. Chen, "Direction-of-arrival estimation using a sparse representation of array covariance vectors," *IEEE Transactions on Signal Processing*, vol. 59, no. 9, pp. 4489–4493, 2011.

[18] S. Lee, Y.-J. Yoon, J.-E. Lee, H. Sim, and S.-C. Kim, "Two-stage DOA estimation method for low SNR signals in automotive radars," *IET Radar, Sonar & Navigation*, vol. 11, no. 11, pp. 1613–1619, 2017.

[19] M. Sun, Y. Wang, and J. Pan, "Direction of arrival estimation by modified orthogonal propagator method with linear prediction in low SNR scenarios," *Signal Processing*, vol. 156, pp. 41–45, 2019.

[20] L. Gan and X. Luo, "Direction-of-arrival estimation for uncorrelated and coherent signals in the presence of multipath propagation," *IET Microwaves, Antennas & Propagation*, vol. 7, no. 9, pp. 746–753, 2013.

[21] R. Schmidt, "Multiple emitter location and signal parameter estimation," *IEEE Transactions on Antennas and Propagation*, vol. 34, no. 3, pp. 276–280, 1986.

[22] P. Stoica and A. Nehorai, "MUSIC, maximum likelihood, and Cramer-Rao bound," *IEEE Transactions on Acoustics, Speech, and Signal Processing*, vol. 37, no. 5, pp. 720–741, 1989.

[23] J. Li, P. Stoica, and Z. Wang, "On robust capon beamforming and diagonal loading," *IEEE Transactions on Signal Processing*, vol. 51, no. 7, pp. 1702–1715, 2003.

[24] S. A. Vorobyov, A. B. Gershman, and Z.-Q. Luo, "Robust adaptive beamforming using worst-case performance optimization: a solution to the signal mismatch problem," *IEEE Transactions on Signal Processing*, vol. 51, no. 2, pp. 313–324, 2003.

[25] Y. Li, H. Ma, D. Yu, and L. Cheng, "Iterative robust capon beamforming," *Signal Processing*, vol. 118, no. 118, pp. 211–220, 2016.

[26] Y. Li, H. Ma, and L. Cheng, "Iterative robust adaptive beamforming," *EURASIP Journal on Advances in Signal Processing*, vol. 58, no. 1, pp. 1–12, 2017.

[27] F.-X. Ge, Q. Wan, J. Yang, and Y.-N. Peng, "A super-resolution time delay estimation based on the MUSIC-type algorithm," *IEICE Transactions on Communications*, vol. 85, no. 12, pp. 2916–2923, 2002.